Dynamic Mobility Spectra of Multicomponent Colloidal Suspensions

Paul J. Bruinsma,* Peter A. Smith,† and Bruce C. Bunker

Pacific Northwest National Laboratory, Mail Stop K8-93, Richland, Washington 99352

Received: March 10, 1997[⊗]

Recently, the electrokinetic sonic amplitude (ESA) signal has been measured over a range of frequencies (collectively termed the dynamic mobility spectrum) for the simultaneous determination of particle charge and size in moderately concentrated suspensions. Based on these advances, we develop theory describing the dynamic mobility spectra for multicomponent suspensions. The dynamic mobility spectrum of multicomponent suspensions can be interpreted as the weighted sum of the individual component dynamic mobility spectra. Weighting coefficients are defined and a methodology for determining these weighting coefficients for binary suspensions with a least-squares technique is developed. Results from multicomponent suspension data are in good agreement with theory. Experimental conditions are restricted to constant pH and ionic strength to avoid changes in the shape of the dynamic mobility spectra of the components, possibly due to agglomeration effects.

1. Introduction

Light scattering is commonly used to determine the mobilities and corresponding zeta potentials of colloidal particles. However, these measurements require dilute suspensions ($\phi \ll 1$ vol %) well below the volume loadings of industrially relevant suspensions. Electrokinetic sonic amplitude (ESA) measurements, in which the mobility is determined from the magnitude of the sonic signal generated from an oscillating electric field applied on the suspension, provides a way for determining the zeta potential of moderately concentrated suspensions[1−4] (0.5−10 vol %).

For particle sizes above ~0.1 μm inertial effects are significant, causing a phase lag and an attenuation of the sonic signal. In the Matec 8000 (Matec Applied Sciences), the ESA signal was measured at a signal frequency. The phase angle, used only for determining the sign of the charge on the particle, was not accurately measured. Therefore, no information could be gained on particle size, unless the zeta potential of the particles was known a priori.

Recently, new equipment was developed, the AcoustoSizer (Matec Applied Sciences), in which the ESA signal is measured over a range of frequencies.[5] The magnitude and the phase shift of the ESA signals are utilized for the simultaneous determination of particle charge and size.

This paper describes the ESA of multicomponent suspensions of the same and different phases. For example, when the mobilities of two suspensions are measured separately, the ESA signal of the combined suspension formed by mixing the two suspensions in known proportions is discussed. Also described is a methodology for the determination of the zeta potentials of individual phases upon mixing by fitting the mobilities of suspensions, comprised of single-particle phases, to the apparent mobilities of the two-component suspensions. In the beginning of the paper, theoretical examples are used to illustrate concepts associated with the equation development. Later, the equations are applied to two-component suspension data, and limitations to the models are discussed.

* To whom correspondence should be addressed. Phone: (509) 376-4638. Fax: (509) 376-5106. E-mail: pj_bruinsma@pnl.gov.

† Current address: Motorola, Tempe, AZ 85284.

⊗ Abstract published in *Advance ACS Abstracts,* October 1, 1997.

2. Dynamic Mobility of Spherical Particles

The motion of a spherical particle of radius, R, due to an imposed electric field is considered for the case of a thin double layer relative to the particle size ($kR > 50$, where $1/k$ is the Debye length). In an oscillating electric field, the electric field is represented by $E_0 \exp(i\omega t)$ and the velocity by $V_0 \exp(i\omega t)$. Therefore,

$$V_0 = \mu_d E_0 \tag{1}$$

where μ_d is the dynamic mobility of the particle, proportional to the zeta potential. At high frequency, the particle velocity can lag behind the oscillating electric field because of the finite particle momentum. Therefore, V_0 and μ_d are generally complex-number quantities.

O'Brien derived the relationship between the dynamic and the electrophoretic mobilities of spherical particles.[1] For thin double layers, the dynamic mobility is related to the electrophoretic mobility by

$$\mu_d = \mu_E \frac{2}{3}(1 + f)G \tag{2}$$

where f accounts for conduction through the double layer[1,6,7] and, in general, has a complex-number value. However, for most suspensions of particles with thin double layers, surface conduction has a negligible effect, as long as the zeta potential is not high.[5,7] Therefore, $f = 1/2$ and eq 2 simplifies to

$$\mu_d = \mu_E G \tag{3}$$

In the equation development below, it is assumed that $f = 1/2$. The function G is dependent on the parameter $\Delta\rho/\rho$ (ρ is the fluid density and $\Delta\rho$ is the density difference between the particle and fluid) and on the variable α, the nondimensional frequency, given by

$$\alpha = \omega R^2 \rho/\mu \tag{4}$$

where ω is the angular frequency of the electric field and μ is the viscosity.

It is instructive to relate the momentum effects of electrophoresis and those of Brownian motion. The characteristic time for the relaxation of the particle momentum (due to a thermal

S1089-5647(97)00892-4 CCC: $14.00

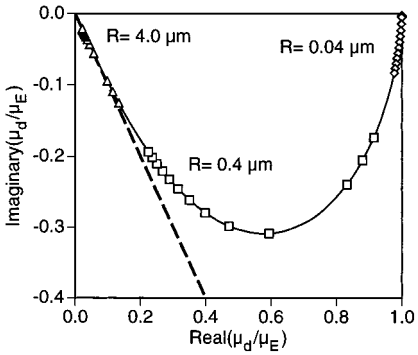

Figure 1. Theorectical dynamic-mobility spectra of different size spherical alumina particles for a set of electric-field frequencies (see text). For a given particle density, the mobility data of different size sphereical particles lie on a characteristic curve.

fluctuation in Brownian motion, for example) is given by[8]

$$\tau_R = m/\zeta = \frac{4}{3}\pi R^3\rho/6\pi\mu R = \frac{2}{9}R^2\rho/\mu \quad (5)$$

where m is the mass of the particle and ζ is the viscous drag. The momentum relaxation time is related to α by

$$\alpha = \frac{2}{9}\omega\tau_R \quad (6)$$

Therefore, in α, the frequency of the applied field is scaled by the momentum relaxation time. Inertia effects are important for larger values of α, and viscous effects dominate for small α values.

In the AcoustoSizer, dynamic mobilities are determined for a set of 13 fixed frequency values of the applied electric field[9] between 0.3 and 11.1 MHz. The set of mobility data is referred to as the *dynamic-mobility spectrum* and can be represented as a series of points on the complex plane. In Figure 1, examples of dynamic mobility spectra calculated from eq 3 (where G is defined in ref 1) are shown for three different size particles where the properties of alumina were assumed for the particle densities. The spectra are normalized by the electrophoretic mobility. For a given particle density, G is a function only of α. Therefore, all of the normalized dynamic-mobility values lie along the characteristic curve on the complex plane, as indicated in Figure 1.

For small particles or low frequency of the applied electric field where $\alpha \ll 1$, the dynamic and static mobilities are identical. Viscous effects dominate, and the mobility is independent of the particle momentum. Although the value of the zeta potential can be determined from the dynamic mobility, the particle size cannot be determined because of the negligible inertial effect.

In the intermediate range, α can be determined from the phase angle of the dynamic mobility. Because the inertial effect is significant but not overwhelming, the dynamic-mobility spectrum is used collectively for calculating the zeta potential, average log-normal particle size, and the size distribution width.[5] The balance between viscous and inertial forces allows particles in the size range 0.1−10 μm to be characterized by the instrument.[10]

For large particles or high frequency where $\alpha \gg 1$, inertial effects dominate,

$$\mu_d/\mu_E = G(\Delta\rho/\rho{:}\alpha) \approx \frac{9/2}{\sqrt{\alpha/2}(3 + 2\Delta\rho/\rho)}(1 - i) \quad (7)$$

The dynamic-mobility data lie near the line with an angle of 45° through the origin of the complex plane, corresponding to the maximum phase lag of the particle. In this limit, the value of G scales with $(1/R)$. Independent values for the particle size and the zeta potential cannot be determined.

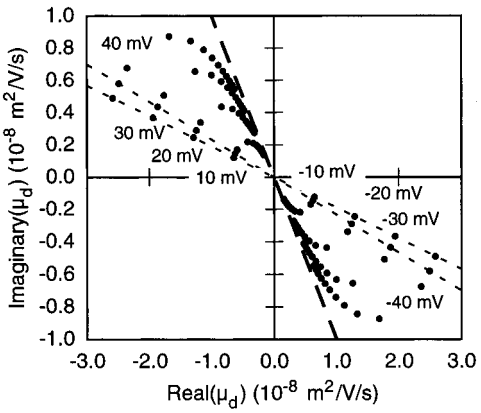

Figure 2. Theorectical dynamic-mobility spectra of 0.4 μm spherical alumina particles for several zeta potential values.

For a given particle size, G is a function only of frequency. Therefore, the phase angle of the dynamic mobility at a given frequency is independent of the zeta potential, and the *shape* of the dynamic spectrum is preserved. Figure 2 shows a series of calculated dynamic-mobility spectra for a 0.4 μm particle for a set of zeta potential values. The plot on the complex plane of the dynamic-mobility spectra with varying solution conditions is referred to as a *star plot*. The dynamic mobilities for a given frequency lie along a straight line passing through the origin.

For a distribution in particle sizes an average mobility can be defined as

$$\langle\mu_d\rangle(\omega) \equiv \int_0^\infty \mu_d(\omega,R)\, p(R)\, dR = \mu_E\int_0^\infty G(\Delta\rho/\rho{:}\alpha(\omega,R))\, p(R)\, dR \quad (8)$$

where $\langle\ \rangle$ denotes the average (or effective) value determined by the instrument and *p(R)* is the particle-size frequency on a mass basis.[5] Because the primary particle sizes in the suspension are assumed not to change, the dynamic mobilities change proportionally to the value of the electrophoretic mobility. Although a log-normal size distribution is assumed for the calculation of the particle size distribution in the AcoutoSizer software, eq 8 indicates the proportionality relationship is more general. In the titration of a suspension with an arbitrary particle-size distribution, a set of dynamic-mobility spectra is produced, all of which are multiples of each other (see Figure 2), assuming no special phenomena occur, such as agglomeration or significant surface conductivity effects.

Along with particle-size distributions, suspensions of industrial importance contain nonspherical particles that produce a characteristic shape of the dynamic-mobility spectrum.[11] In section 3, the process is described that shows how the spectra of component suspensions form the spectrum for the multicomponent suspension. Subsequently, it is shown how the component spectra can be fit to the two-component suspension spectrum to determine the zeta potential changes of each particle phase.

3. ESA of Multicomponent Suspensions

The dynamic-mobility spectrum of a multiphase suspension is readily determined. The multiphase suspension is poured into the cell of the main sensor unit just as for a pure phase suspension. The volume fraction and density can be entered as the total volume fraction and an average density of the two particle phases. A measurement is made, and the instrument

reports values for the dynamic mobility with frequency without regard to the mixed nature of the suspension. Rather than in the measurement, the difficulty is in the interpretation and the understanding of the dynamic mobility results.

For single-phase suspensions with monosize particles, the dynamic mobility has a specific meaning as a transport property, given by eq 1. However, the term is also used here more loosely as the value reported by the instrument. Even for single-phase suspensions with particle-size distributions of finite width, the so-called *average* dynamic mobility does not have a straightforward relationship to transport properties. Instead, the average, as defined in eq 8, corresponds to that determined with the instrument.

In sections 3.1 and 3.2, equations are derived for the dynamic mobility spectra in which the particles are composed of the same phase and of different phases. In section 3.3, weighting coefficients are defined for the addition of the dynamic mobility spectra of the individual phases. The ESA of suspensions with more than two phases is discussed in section 3.4.

3.1. Two-Component, Same-Phase Suspensions. As a simple case, consider the dynamic-mobility spectrum for a mixture of two suspensions of spherical particles with different size distributions, but of the same phase. The size distribution of a suspension consisting of a single particulate phase, comprised of two discrete particle sizes, is

$$p_{\mathrm{mix}}(R) = \mathrm{x}_1 p_1(R) + (1 - \mathrm{x}_1) p_2(R) \tag{9}$$

where x_1 is the solids mass fraction of the first particle type in the mixture. From eq 8, the dynamic mobility of the mixture is

$$\langle \mu_{\mathrm{d}} \rangle_{\mathrm{mix}}(\omega) = \mu_{\mathrm{E}} \int_0^\infty G(\Delta\rho/\rho{:}\alpha(\omega,R))\, p_{\mathrm{mix}}(R)\, \mathrm{d}R \tag{10}$$

Substituting with the expression for the size distribution,

$$\langle \mu_{\mathrm{d}} \rangle_{\mathrm{mix}}(\omega) = x_1 \mu_{\mathrm{E}} \int_0^\infty G(\Delta\rho/\rho{:}\alpha(\omega,R))\, p_1(R)\, \mathrm{d}R + (1 - x_1) \mu_{\mathrm{E}} \int_0^\infty G(\Delta\rho/\rho{:}\alpha(\omega,R))\, p_2(R)\, \mathrm{d}R \tag{11}$$

which simplifies to

$$\langle \mu_{\mathrm{d}} \rangle_{\mathrm{mix}}(\omega) = x_1 \langle \mu_{\mathrm{d}} \rangle_1(\omega) + (1 - x_1) \langle \mu_{\mathrm{d}} \rangle_2(\omega) \tag{12}$$

Thus, the mobility for the mixture is a weighted sum of the mobilities of the two components. Alternatively, eq 12 can be written as

$$\phi_{\mathrm{mix}} \langle \mu_{\mathrm{d}} \rangle_{\mathrm{mix}}(\omega) = \phi'_1 \langle \mu_{\mathrm{d}} \rangle_1(\omega) + \phi'_2 \langle \mu_{\mathrm{d}} \rangle_2(\omega) \tag{13}$$

where ϕ'_1 and ϕ'_2 are the volume fractions of particle types 1 and 2 in the two-component suspensions, and the primes denote the value in the mixture. The total volume fraction of the two-component suspension is

$$\phi_{\mathrm{mix}} \equiv \phi'_1 + \phi'_2 \tag{14}$$

Due to the fact that dynamic mobility contains both real and imaginary parts, eq 13 is a weighted average of complex values.

The combination of two dynamic-mobility spectra to form the spectrum of the mixture is illustrated in Figure 3. In the example, the component spectra were calculated for 0.20 and 0.60 μm spherical alumina particles with a zeta potential of 25 mV and respective volume fractions of $\phi'_1 = 0.05$, $\phi'_2 = 0.04$, and a total volume fraction of 0.09. On the plot, the dynamic-mobility spectra are each weighted by their respective volume fractions in the mixture. The addition of the component spectra can be represented by vector addition on the complex plane.

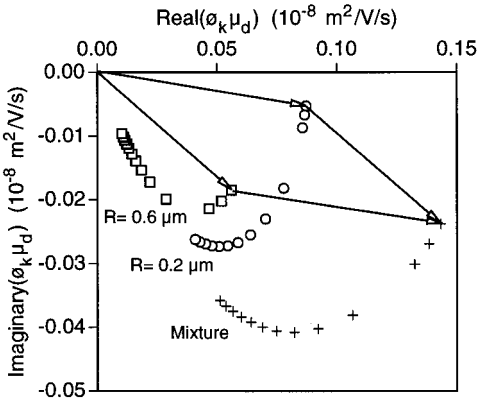

Figure 3. Illustration of the addition of the dynamic-mobility spectra of the component suspensions to form the dynamic-mobility spectrum of the mixture. Theorectical dynamic-mobility spectra were calculated for spherical alumina particles with 0.60 and 0.2 μm radii and a zeta potential of 25 mV.

This approach is similar to that of Desai[12] in which vectors represented the subtraction of the background contribution of the electrolyte to the ESA signal.

3.2. Two-Phase Suspensions. In more general problems, a similar weighted addition is used to calculate the dynamic-mobility spectra of multiple-phase and nonspherical-particle suspensions. Before addressing the former, the measurement technique is reexamined. The strength of the ESA is related to the dynamic mobility of a suspension consisting of a distribution of sizes by

$$\mathrm{ESA} = \phi \frac{\Delta\rho}{\rho} \langle \mu_{\mathrm{d}} \rangle A(\omega) E \tag{15}$$

where ϕ is the volume fraction of the particulate phase and $A(\omega)$ is a constant that includes an instrument constant and the impedances of the sample and glass rod.[5]

The ESA signal of the two-component suspension is given by

$$\mathrm{ESA} = \left[\phi'_1 \frac{\Delta\rho_1}{\rho} \langle \mu_{\mathrm{d}} \rangle'_1 + \phi'_2 \frac{\Delta\rho_2}{\rho} \langle \mu_{\mathrm{d}} \rangle'_2 \right] A(\omega) E \tag{16}$$

where the prime denotes the value in the mixture. Note the acoustic impedances can vary from one sample to another. However, the sample acoustic impedances are determined during each dynamic-mobility measurement.[5]

The mobility of each component in the two-component suspension is given by

$$\langle \mu_{\mathrm{d}} \rangle'_k(\omega_j) = \frac{\zeta'_k}{\zeta_k} \langle \mu_{\mathrm{d}} \rangle_k(\omega_j) \tag{17}$$

In eq 17, the ratio of the zeta potentials in the mixture and the pure suspension allows for changes in the zeta potential. For example, ions may desorb from one phase and adsorb onto the second phase. Although the zeta potential may change, it is assumed that the shape of the dynamic-mobility spectrum, given by the G function, will be preserved in the absence of significant changes in the mass of the particles. From these assumptions, the dynamic mobility for the mixture is defined as

$$\phi_{\mathrm{mix}} \frac{\Delta\rho_{\mathrm{mix}}}{\rho} \bar{\mu}_{\mathrm{d_{mix}}} \equiv \phi'_1 \frac{\Delta\rho_1}{\rho} \langle \mu_{\mathrm{d}} \rangle'_1 + \phi'_2 \frac{\Delta\rho_2}{\rho} \langle \mu_{\mathrm{d}} \rangle'_2 \tag{18}$$

where the volume fraction of the two-component suspension is given by

$$\phi_{\mathrm{mix}} \equiv \phi'_1 + \phi'_2 \tag{19}$$

and the density by

$$\rho_{mix} \equiv (\phi'_1/\phi_{mix})\rho_1 + (\phi'_2/\phi_{mix})\rho_2 \quad (20)$$

The choice for the definition of the density of the two-component suspension is somewhat arbitrary. However, the definitions of the two-component density and two-component mobilities are linked because the density is used in the calculation of the dynamic-mobility values.

The term *dynamic mobility of the two-component suspension* means the mobility values that would be determined for the suspension mixture. This term is not intended to define a variable equivalent to an *average zeta potential* that could be used to predict or interpret suspension properties, such as rheological behavior.

However, for the case when the zeta potentials of a mixed particle system are equal (when one phase coats the other phase, for example) and in the limit of negligible inertia effects, the mixture density, as defined in eq 20, will yield a correct zeta potential value. This result can be verified by substituting the definition of the density of the two-component suspension into eq 18.

3.3. Weighting Coefficients. By rearranging eq 18, the following real-number coefficients can be defined:

$$a \equiv \left(\frac{\zeta'_1}{\zeta_1}\right)\left(\frac{\phi'_1\Delta\rho_1/\rho}{\phi_{mix}\Delta\rho_{mix}/\rho}\right) \quad (21)$$

$$b \equiv \left(\frac{\zeta'_2}{\zeta_2}\right)\left(\frac{\phi'_2\Delta\rho_2/\rho}{\phi_{mix}\Delta\rho_{mix}/\rho}\right) \quad (22)$$

Therefore, eq 18 can be written as the weighted average of the two measured acoustic spectra of the component phases:

$$\bar{\mu}_{d_{mix}}(\omega) = a\langle\mu_d\rangle_1(\omega) + b\langle\mu_d\rangle_2(\omega) \quad (23)$$

In the case when two suspensions of the same particle phase (but perhaps different particle sizes) are combined and where the zeta potential and density are constant, *a* and *b* give the volume contribution of solid from each suspension to the mixed suspension. For example

$$a = \frac{\phi'_1}{\phi_{mix}} = \frac{v_1/(v_1 + v_2 + v_L)}{(v_1 + v_2)/(v_1 + v_2 + v_L)} = \frac{v_1}{(v_1 + v_2)} \quad (24)$$

where v_1 is the volume of solids from the first suspension, v_2 is the volume of solids from the second suspension, and v_L is the liquid volume.

In section 4.1, fitting the coefficients *a* and *b* using a least-squares technique is discussed. In cases where the dynamic-mobility spectra of the two pure suspensions are similar (the average particle sizes are similar to each other), it is difficult to obtain accurate fits for the coefficients. However, by comparing the mobility data of the mixture to that of the pure suspensions using eq 23, it is possible to evaluate whether interaction occurs between the two particle phases. For the case where no interaction is present between the two phases (that is, unvarying zeta potentials), eq 23 will predict the mobility spectrum of the mixture when *a* and *b* values are calculated using constant zeta potentials. If the particles of suspension 1 are soluble and reprecipitation occurs onto the particles of suspension 2, a better prediction will be obtained by calculating *a* and *b* values using the zeta potential of suspension 1 for that of suspension 2 in the mixture.

3.4. Multiple-Phase Suspension Mixtures. For several particle sizes and phases, the volume fraction of the mixture is defined as

$$\phi_{mix} = \sum_{k=1}^{K} \phi'_k \quad (25)$$

and the density of the mixture is defined as

$$\rho_{mix} = \frac{1}{\phi_{mix}}\sum_{k=1}^{K} \phi'_k\rho_k \quad (26)$$

The dynamic mobility of the mixture is

$$\bar{\mu}_{d_{mix}}(\omega) = \frac{\sum_{k=1}^{K} \phi'_k\Delta\rho_k(\zeta'_k/\zeta_k)\int_0^\infty \mu_{d_k}(\omega,R)\, p_k(R)\, dR}{\sum_{k=1}^{K} \phi'_k\Delta\rho_k} \quad (27)$$

where μ_{d_k}, ϕ_k, and ρ_k are the dynamic mobility, volume, and the density of the *k*th particle type, respectively.

In section 4.1, equations are given for the calculation of the *a* and *b* weighting coefficients, from which the zeta potentials of each individual phase can be determined. In principle, these equations can be extended to more components. However, it is unlikely the instrument will have sufficient resolution to determine the zeta potentials of more than two individual phases. Instead, eq 27 is useful for describing the contribution of each phase to the mixed suspension mobility spectrum. This description is predicated on either unchanged zeta potentials in the multicomponent suspension or on a priori knowledge of the zeta potential of each phase within the mixed-phase suspension.

4. Least-Squares Fits for Dynamic-Mobility Spectra[13]

The values of the coefficients *a* and *b* can be determined by fitting the single-component spectra to the two-component suspension spectrum, as will be shown. The values of *a* and *b* allow the determination of zeta potentials for each phase when the surface charges of the components are modified as a result of combining the two phases. It should be noted that a least-squares minimization technique is also the basis for the calculation of the zeta potential and size distribution in the AcoustoSizer software.[5]

4.1. Calculation of Weighting Coefficients for Binary Suspensions. Let *A* be a set of dynamic-mobility data for pure suspension 1 measured at a set of fixed frequencies, ω_1, ..., ω_j, ..., ω_M. Therefore,

$$A_j(\omega_j) \equiv \langle\mu_d\rangle_1(\omega_j) = |A_j|[\cos(\alpha_j) + i\sin(\alpha_j)] \quad (28)$$

where $|A_j|$ and α_j are the magnitude (or modulus) and phase angle (or argument) of A_j. In eq 28, *A* is referred to as the dynamic-mobility spectrum of suspension 1. Note the dynamic-mobility spectra consist of sets of complex numbers which can be expressed as magnitudes and phase angles. In the context of the dynamic mobility literature, the magnitude can assume either positive or negative values and, typically, the phase angles have ranges from $-\pi/2$ to 0. The dynamic mobilities of porous flocs can have phase angles outside of this range.[14] However, only dispersed suspensions are considered here.

Let *B* and *C* be the dynamic-mobility spectra of suspension 2 and of the two-component suspension, respectively. The dynamic-mobility spectrum of the suspension mixture is modeled as the weighted sum of the pure-suspension dynamic-mobility spectra. Therefore,

$$C_j^{model} = aA_j + bB_j \quad (29)$$

The error in the model is given by

$$D_j = C_j - C_j^{\text{model}} = C_j - aA_j - bB_j \tag{30}$$

Below, the subscripts on a_0 and b_0 denote the values of a and b that yield a minimum in the sum of the squares of the residuals between the model and the measured two-component suspension spectrum (see the Supporting Information). Because of instrument imprecisions and deviations from linear theory, a finite error will exist. Using a least-squares technique, the values of the coefficients a_0 and b_0 are given by

$$a_0 = \frac{[AB][BC] - [B^2][AC]}{[AB]^2 - [A^2][B^2]} \tag{31}$$

$$b_0 = \frac{[AB][AC] - [A^2][BC]}{[AB]^2 - [A^2][B^2]} \tag{32}$$

where the following shorthand is used for representing the summations:

$$[XY] = \sum_{j=1}^{M} w_j |X_j||Y_j| \cos(x_j - y_j) \tag{33}$$

$$[X^2] = \sum_{j=1}^{M} w_j |X_j|^2 \tag{34}$$

involving two dynamic mobility spectra, X and Y, with magnitudes $|X_j|$ and $|Y_j|$ and phase angles x_j and y_j, respectively. The real-number weighting factor, w_j, can be used to account for variations in the precision at each frequency. The weighting factors are included here and in the Supporting Information for completeness, but are set to 1 in section 6 for simplicity. It should be recognized that $[XY]$ and $[X^2]$ represent real-number values. The sum of the squares of the residuals between the model and the measured spectra is given by

$$S_r = [C^2] - a_0[AC] - b_0[BC] \tag{35}$$

The value of S_r provides a measure of how well the two-component suspension mobility data are fit by eq 29.

4.2. Sensitivity for the Values of the Weighting Coefficients. It is important to consider the sensitivity to the calculated a and b values. If the a and b values could be changed by large amounts with only a correspondingly small increase in the residual error, there would be little confidence in the calculated values. Defining the differences between the a and b values from those calculated by eqs 31 and 32 as δa and δb, respectively, the increase in the sum of the squares of residual error, ΔS_r, is

$$\Delta S_r = [A^2](\delta a)^2 + 2[AB]\delta a\, \delta b + [B^2](\delta b)^2 \tag{36}$$

For fixed values of ΔS_r, eq 36 defines a series of rotated ellipses on the $\delta a - \delta b$ plane. For a constant ΔS_r value, generally the a and b coefficients can be changed by greater amounts when one is increased and the other is decreased. Normalizing δa and δb by

$$\delta a' = \sqrt{[A^2]}\, \delta a \tag{37}$$

$$\delta b' = \sqrt{[B^2]}\, \delta b \tag{38}$$

eq 41 can be rewritten as

$$\Delta S_r = (\delta a')^2 + 2\frac{[AB]}{\sqrt{[A^2][B^2]}}\, \delta a'\, \delta b' + (\delta b')^2 \tag{39}$$

The coefficient term on $\delta a'\, \delta b'$ in eq 39 ranges between -2 and 2, depending on the component mobility spectra. The closer the term is to 2 or to -2, the more elongated the ellipse becomes and the greater the range of δa and δb values.

The size of the ellipse is dependent on ΔS_r. The value of ΔS_r that should be chosen in a particular set of experiments is not yet resolved. Certainly, the expected repeatability of the mobility spectrum measurement needs to be taken into account. In addition, changes in the electrolyte concentration with pH adjustment, for example, can have subtle effects on the shape of the mobility spectrum. In turn these effects influence how accurately the pure suspension mobilities can be fit to the mobilities of the suspension mixture.

In the following section, calculation of the variance for repeated mobility spectrum measurements is discussed. In section 4.4, two mobilities are related with a single constant. This fitting routine can be applied to compare the mobilities of a single-component suspension, when the solution conditions such as pH or electrolyte concentration are varied. The measured variance in the fit of the mobility spectra over a range of solution conditions can give an estimate of the variance for the two-component suspension mobilities.

4.3. Variance in the *A* Data. The precision or repeatability of the dynamic-mobility values can be estimated by repeated measurements on a suspension. The average variance of the repeated measurements is

$$|D_j'|^2 = \frac{\sum_{n=1}^{N} |A_{jn} - \bar{A}_j|^2}{(N-1)} \tag{40}$$

where $\bar{A}_j$ is the average dynamic-mobility data of a set of multiple runs for a suspension and $\bar{A}_{j_n}$ is the data of a particular run, n, at a frequency ω_j. The summation is over the run numbers. With appropriate approximations, the total variance summed over all frequencies is given by

$$\sum_{j=1}^{M} |D_j'|^2 = \left\{ \sum_{j=1}^{M} \left[\left|\bar{A}_j\right|^2 \frac{\pi^2}{180^2} \sum_{n=1}^{N} (\Delta\theta_{j_n})^2 \right] + \sum_{j=1}^{M} \left[\sum_{n=1}^{N} (\Delta A_{j_n})^2 \right] \right\} \Big/ (N-1) \tag{41}$$

where ΔA_{j_n} and $\Delta\alpha_{j_n}$ are the deviations in the magnitude and the phase angle (expressed in degrees) from that of the average data, $\bar{A}_j$. The average variance for suspensions can be compared to the fit error for the suspension mixtures. The influence of deviations in the phase angles and magnitudes on the variance can be determined from eq 41.

4.4. Independence of Two Dynamic-Mobility Spectra. In this section, two dynamic-mobility spectra A and B are compared to see how well they fit the model,

$$B_j = aA_j \tag{42}$$

in which the two spectra are related by a single constant, a. The error is given by

$$D_j'' = aA_j - B_j \tag{43}$$

The constant a_0 is found by minimizing the sum of the squares of the errors. Therefore,

$$a_0 = \frac{[AB]}{[A^2]} \tag{44}$$

The sum of the squares of the errors, normalized by the sum of the squares of the magnitude of spectrum *B*, is given by

$$\frac{[D''^2]}{[B^2]} = 1 - \frac{[AB]^2}{[A^2][B^2]} \tag{45}$$

The ratio on the right-hand side of the equation also appears in eq 39. When the ratio is equal to 1, the mobility spectra, *A* and *B*, can be related by a single proportionality constant. The further the ratio is from 1, the more distinct the two spectra are. Note the terms in the ratio also appear in the denominators for a_0 and b_0 in eqs 31 and 32. When the ratio approaches 1, the denominator approaches zero. Thus, the calculations of a_0 and b_0 will be based on small differences in the numerator terms, and poor accuracy is expected. Equation 45 is used below in section 6.2 as a measure of the change in the shape of the dynamic-mobility spectrum during a titration.

Equation 45 is useful for comparing the dynamic-mobility spectra of two suspensions to be used in the study of a suspension mixture. If the error in fitting the two spectra to each by a constant is small (because of similar particle size distributions for example), little hope exists for separating the contribution of each suspension to the dynamic-mobility spectrum of the mixture.

5. Experimental Section

Gibbsite powder (S-3 grade) was obtained from Alcoa Chemical, and alumina powders (AKP-50 and AKP-15) were obtained from Sumitomo Chemical. Particle size distributions of dilute suspensions were characterized by light scattering using Microtrac Series-9200 (Leeds and Northrup Instruments). Sodium hydroxide, sodium nitrate, and nitric acid were obtained from Aldrich. The 18 MΩ water was obtained from a Millipore Milli-Q Plus ion-exchange unit with a Mill-RO 10 Plus reverse osmosis system. Suspensions were sonified with a Branson Model-450 sonifier. For comparison with electroacoustic measurements, zeta potentials were determined with a Brookhaven Instruments ZetaPlus. Suspensions were diluted with supernatant liquids obtained by centrifugation.

Dynamic-mobility measurements were made with a Matec Applied Sciences AcoustoSizer with an applied field of 1 kV/m over 13 fixed frequencies ranging from 0.3 to 11.5 MHz. The main sensor unit is equipped with conductivity, temperature, and pH probes and a variable speed impeller. The instrument was operated using Singlpt 1.07 software. The principles of operation and calibration of the instrument are described elsewhere.[5]

6. Results and Discussion

6.1. Characterization of Particle Size and Surface Charge. Results for the characterization of the surface charges and particle size distributions are summarized in Table 1. Because both alumina suspensions are composed of high-purity particles and are at nearly identical solution conditions, the zeta potentials are expected to be nearly identical; this is true for the light scattering data. However, the zeta potentials determined with the ESA instrument for the AKP-15 suspension appear to be high. The difference from that of the electrophoretic measurement is not simply due to the limitations in the models accounting for particle inertial effects. Surprisingly, the magnitude of the dynamic mobility measured at the lowest electric field frequency (0.3 MHz) is greater for the AKP-15 than for the AKP-50 suspension (5.77×10^{-8} versus 4.06×10^{-8} m^2 V^{-1} s^{-1}, respectively), although the average particle size of the former is larger, and attenuation by inertial effects should be greater.

Size distributions determined by light scattering are well-represented by log-normal particle distributions; that is, bimodal or multimodal type distributions were not observed. The log-normal size distributions determined with the ESA instrument are in reasonable agreement with the log-normal size distributions fit to the light scattering, especially when considering the typically nonspherical nature of particles within commercial-grade powders.

The dynamic mobility spectrum of the AKP-15 suspension was fit for a bimodal particle-size distribution

$$A_j = \frac{\epsilon}{\mu}[x_1 G(\alpha_j(r_1)) + (1 - x_1) G(\alpha_j(r_2))] \tag{46}$$

where x_1 is the mass fraction of particles of radius r_1 and $(1 - x_1)$ is the mass fraction of particles of radius r_2 (details of the fitting method is provided in the Supporting Information). The particle size distribution was calculated to be 53.5% by the mass of the particles with a diameter of 0.50 μm, with the remainder 1.34 μm in diameter and the zeta potential of 89.1 mV. The theoretical dynamic mobilities for the bimodal and the log-normal particle-size distributions are well-matched to the dynamic-mobility data; the residual errors calculated with eq 45 were 6×10^{-5} and 8×10^{-5}, respectively. However, the particle-size distribution obtained by light scattering was not consistent with a bimodal particle size distribution. This problem illustrates those difficulties associated with fitting mobility data to unique size distributions.

6.2. Gibbsite Star Plot. A 5 vol % gibbsite suspension with an added electrolyte of 0.001 M NaNO3 was prepared initially at pH 4 and was titrated with NaOH solution. Figure 4 shows the *star plot* of dynamic mobilities of the gibbsite suspension measured with increasing pH through the isoelectric point (iep). Ideally, the phase angles at each frequency would remain constant. At the lowest and highest frequency values, the phase angle changes from 11.3 and −30.7 to −11.9 and −39.0, respectively. Figure 5 shows the error in the fit given by eq 45. The error would be zero for the case when the dynamic mobility spectra are related by a constant. The shapes of the dynamic mobility spectra change in a continuous manner, and the error increase is not attributed to simply random measurement error due to reduced signal strength as the iep is approached. Measurements of the ESA responses of KSiW electrolyte standards[5] with conductivities ranging from 0.025 to 0.76 S/m show negligible instrument precision errors.

It is speculated that the changes in the shape of the dynamic-mobility spectrum may be due to subtle changes in the suspension microstructure due to the effects of agglomeration as the iep is approached. The error for the gibbsite suspension increases monotonically as the iep is approached and decreases past the iep. It may be expected that agglomeration would show a more abrupt change as the magnitude of the surface charge is decreased below the limit of stability. However, the concentrated suspension is initially quite opaque, indicating some degree of flocculation from the start of the titration. To our knowledge no experimental study exists for effects of agglomeration on the ESA signal, and theory is currently limited to highly idealized flocs.[14]

In general, several phenomena are of concern as the suspension approaches the iep: (a) sedimentation, (b) interference caused by adherence of the suspension particles onto the electrode surface, (c) domination of the ESA signal by the background electrolyte contribution,[5] and (d) changes in the

TABLE 1[a]

	vol %	pH	cond (S/m)	light scatter. (mV)	ESA (mV)	light d50 (μm)	light d16 (μm)	light d84 (μm)	ESA d50 (μm)	ESA d16 (μm)	ESA d84 (μm)
gibbsite	5	4.04	0.126	n/a	78.6	1.56	0.83	2.9	1.04	0.45	2.41
AKP−50 alumina	5	4.21	0.078	81.8 ± 4.8	77.3	0.26	0.18	0.38	0.12	0.038	0.39
AKP−15 alumina	3	4.28	0.085	79.8 ± 9.3	93.9	0.45	0.33	0.62	0.58	0.32	1.04

[a] For example, 16% of the particle-size distribution by mass has a diameter below the d16 value.

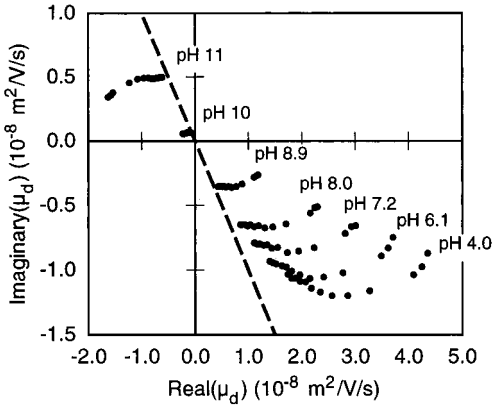

Figure 4. Dynamic mobility spectra of a 5 vol % gibbsite suspension titrated with NaOH. The phase angles decrease with the magnitude of the zeta potential due to instrument problems at low ESA signal strengths. The dashed line at 45° shows the phase lag limit for spherical particles.

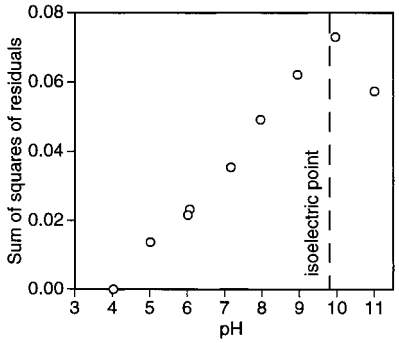

Figure 5. Square of the residuals (see eq 35) between the dynamic-mobility spectrum measured at pH 4.04 and the spectra measured with increasing pH.

double layer and surface conduction as the surface charge is decreased. Sedimentation could cause a decrease in the effective particle volume fraction in the sensing zone. However, sedimentation would change the shape of the dynamic-mobility spectrum only by modifying the particle-size distribution. The phase lag increases as the iep is approached, and the apparent average particle size is larger, which is inconsistent with preferential sedimentation of larger particles. No significant sedimentation or adherence of particles onto the electrode surface was observed in the experiment. The mixing was sufficient to prevent both of these effects. Correction of dynamic-mobility spectra for the electrolyte contribution[5] to the ESA signal has a negligible effect because sodium nitrate has a weak electroacoustic signal. Addition of sodium nitrate to a gibbsite suspension at pH 4 (high zeta potential value) has a strong effect on the shape of mobility spectrum but does not produce the same trend of changes observed in the pH titration. Therefore, the shape changes cannot solely be due to surface conduction effects.

To avoid problems associated with changes in the dynamic-mobility spectra, the pH and salt concentrations will be maintained constant in the mixed suspension systems discussed below.

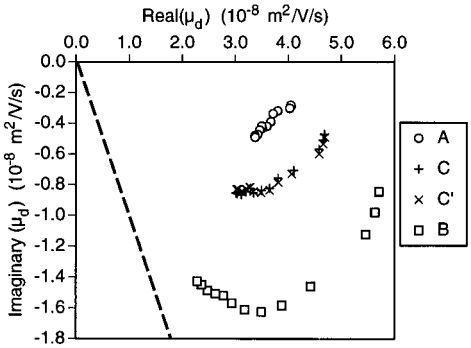

Figure 6. Dynamic-mobility spectra of (A) 5 vol % AKP-50 alumina, (B) 3 vol % AKP-15 alumina, and (C) the mixed-phase suspensions. The fitted dynamic mobility spectrum (C′) is also shown.

6.3. Alumina Suspension Mixture. Two alumina suspensions (5 vol % AKP-50 and 3 vol % AKP-15) were prepared at pH 4.29 ± 0.06 with an initial added electrolyte of 0.002 M NaNO3. Particle size and surface charge characterization of the suspensions were discussed previously. Repeated measurements (at least four times) of the dynamic mobilities of the single-component and two-component suspensions were made. The size of the variances, expressed as

$$\sqrt{\sum_{j=1}^{M}|D_j'|^2/\sum_{j=1}^{M}|\bar{A}_j|^2} \times 100\% \qquad (47)$$

were 0.54, 0.21, and 0.28% for the first, second, and mixed alumina suspensions, respectively. The variability in the magnitude and phase angle values have roughly the same contribution to the variance.

The suspension mixture was formed by combining the first and second suspensions and recording the mass of each. From the masses, the total volume fraction of solids was calculated to be 4.03 vol %. The dynamic mobilities of the pure component and two-component suspensions are shown in Figure 6. The larger phase lags and imaginary values for the mobilities of the AKP-15 powder are consistent with its larger particle size. The mobilities of the two-component suspension are shown as an average of the two-component suspensions in Figure 6. The *a* and *b* weighting coefficients were calculated from eqs 31 and 32 to be 65.4 and 35.7%, which are in close agreement to the expected values of 63.9% of the solids from the first suspension and 36.1% from the second, calculated from the mass contribution of each suspension. The latter values represent the volume contribution of solids from the first and second suspension to the two-component, same-phase suspension (see eq 24). Also shown in Figure 6 is the dynamic mobility spectrum calculated from eq 23 using the fitted *a* and *b* values from the individual alumina suspensions.

Although the *a* and *b* values are close to the expected values, the error is finite. It is helpful to examine the possible source of error in more detail. Possibly, the error can be attributed to the limited precision of the dynamic mobility measurements. By assigning an allowable increase in the sum of the residual error due to instrument precision, ΔS_r, in eq 36 to a weighted sum of the suspension mobility variances (see eq 41),

$$\Delta S_r = a_0^2(\sum_{j=1}^{M}|D_j'|^2)_A + b_0^2(\sum_{j=1}^{M}|D_j'|^2)_B + (\sum_{j=1}^{M}|D_j'|^2)_C \quad (48)$$

the range of δa and δb values can be determined (see section 4.2). This range of values associated with instrument precision is represented in Figure 7 by an ellipse. The point represents the δa, δb values for the difference between the expected and fitted a, b values and is well outside the ellipse. Therefore, the error is not attributed to the limited precision of the instrument.

Instead, the difference between the expected and fit a, b values may be due to actual changes in the charges of the particles. The differences correspond to relatively small changes in the zeta potentials of the particles of the first and second suspensions of −1.8 and 0.8 mV, respectively, which can be caused by pH changes on the order of 0.20. Actual differences in the pH values were on the order of 0.10, because the pH values of the suspensions were not perfectly adjusted. An additional source for the error may be deviations from linear theory that are not well-understood or explored.

6.4. Two-Phase Suspension. Two suspensions were prepared: one containing 5 vol % gibbsite and the second with 4 vol % AKP-50 alumina with added electrolyte concentrations of 0.004 M $NaNO_3$. The two phases have very different densities (2.42 and 3.97 g/cm^3, respectively). The solution chemistries of the two suspensions are similar as both are composed of alumina phases, and changes in the surface charges upon mixing would not be expected. Therefore, the mixture provides a good test for eq 18, which describes the two-phase suspension dynamic mobility. Initially, the dynamic-mobility spectrum of gibbsite was measured at pH 5.3 and a conductivity of 0.1 S/m. The conductivity was higher than would be expected for the added electrolyte alone, presumably due to partial dissolution of the gibbsite.

The pH and conductivity of the alumina suspension was adjusted to the same pH and conductivity of the gibbsite suspension, and the dynamic-mobility spectrum was measured. The two suspensions were combined in known mass amounts, and the mobility of the two-phase suspension was measured.

By substituting the dynamic mobilities of the gibbsite, alumina, and two-phase suspensions into eqs 31 and 32, the a and b weighting coefficients for gibbsite and alumina were calculated to be 0.34 and 0.69, respectively. These values are in agreement with the values of 0.33 and 0.66 calculated from eqs 21 and 22 using the known fraction of each phase in the mixed suspension and assuming constant zeta potentials. In the plot of the dynamic-mobility spectra (not shown for brevity), the calculated dynamic-mobility spectrum is in good agreement with the measured dynamic-mobility spectrum of the two-phase suspension.

7. Conclusions

The ESA of suspension mixtures can be interpreted as the weighted sum of the individual component dynamic-mobility spectra. Weighting coefficients are defined and a methodology is developed to determine these weighting coefficients for binary suspensions with a least-squares technique. Results from suspension−mixture data were in agreement with theory. However, the experimental conditions were restrictive; the pH and ionic strength were kept constant to avoid problems with changes in the shape of the dynamic-mobility spectra of the components, possibly due to agglomeration effects. Although the influence of these changes on average particle size with the AcoustoSizer is negligible, it can cause significant errors in the determination of the weighting coefficients. Further use of the theory is dependent on improved understanding of the pH response of the suspensions.

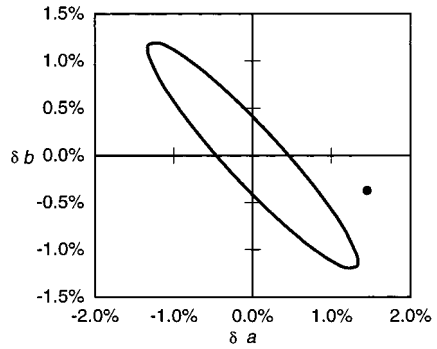

Figure 7. Ellipse indicating the region in which the differences in values of the a and b weighting coefficients away from the expected values are consistent with finite instrument precision. The filled circle represents the difference between the expected a and b weighting coefficients and those found by fitting the dynamic-mobility spectra. Since the point is outside the ellipse, the differences between the expected and calculated a and b values are not attributed to limited instrument precision.

Acknowledgment. P.J.B. was supported in this research by Associated Western Universities, Inc., Northwest Division, under Grant DE-FG06-92RL-12451 with the U.S. Department of Energy. Additional support was provided by the Radiocolloids Laboratory operated by Pacific Northwest National Laboratory. Pacific Northwest National Laboratory is operated for the U.S. Department of Energy by the Battelle Memorial Institute under Contract DE-AC06-76RLO 1830.

Supporting Information Available: Detailed derivations of the equations (8 pages). Ordering information is given on any current masthead page.

References and Notes

(1) O'Brien, R. W. *J. Fluid Mech.* **1988**, *190*, 71.
(2) O'Brien, R. W.; Midmore, B. R.; Lamb, A.; Hunter, R. J. *Faraday Discuss. Chem Soc.* **1988**, *90*, 301.
(3) O'Brien, R. W. *J. Fluid Mech.* **1990**, *212*, 81.
(4) O'Brien, R. W.; White, L. R. *J. Chem. Soc., Faraday Trans. 2* **1978**, *74*, 1607.
(5) O'Brien, R. W.; Cannon, D. W.; Rowlands, W. N. *J. Colloid Interface Sci.* **1995**, *173*, 406.
(6) O'Brien, R. W. *J. Colloid Interface Sci.* **1986**, *113*, 81.
(7) Rowlands, W. N.; O'Brien, R. W. *J. Colloid Interface Sci.* **1995**, *175*, 190.
(8) Keiser, J. *Statistical Thermodynamics of Nonequilibrium Processes*; Springer-Verlag: New York, 1987; p 33.
(9) The dynamic mobilities are measured at frequencies of 0.30, 0.40, 0.54, 1.6, 2.7, 3.7, 4.8, 5.9, 6.9, 8.0, 9.0, 10.1, and 11.1 MHz. In the theoretical examples illustrated in Figures 1-3, the set of frequency values is used to calculate the mobilities.
(10) *Matec AcoustoSizer User's Manual*; Matec Applied Sciences: Hopkinton, MA, July 1995; p 2.1.
(11) Loewenberg, M.; O'Brien, R. W. *J. Colloid Interface Sci.* **1992**, *150*, 158.
(12) Desai, F. N.; Hammad, H. R.; Hayes, K. F. *Langmuir* **1993**, *9*, 2888.
(13) The equations presented in section 4 are discussed in more detail in the Supporting Information.
(14) Miller, N. P.; Berg, J. C.; O'Brien, R. W. *J. Colloid Interface Sci.* **1992**, *153*, 237.